

SELENIDE AND TELLURIDE THICK FILMS FOR MID AND THERMAL INFRARED APPLICATIONS

C. Vigreux-Bercovici*, L. Labadie^a, J.E. Broquin^b, P. Kern^a, A. Pradel

Laboratoire de Physico-chimie de la Matière Condensée, Institut Gehrhardt, UMR 5617, Université Montpellier II, Place Eugène Bataillon, 34095 Montpellier cedex 5, France

^aLaboratoire d'Astrophysique de l'Observatoire de Grenoble, Observatoire de Grenoble, BP 53, 38041 Grenoble cedex 9, France

^bInstitut de Microélectronique, Electromagnétisme et Photonique, ENSERG, 23 av. des Martyrs, BP 257, 38016 Grenoble cedex 1, France

Planar waveguides based on selenide (As_2Se_3) or telluride (TeAs_4Se_5 or $\text{Te}_2\text{As}_3\text{Se}_5$) glasses were elaborated and shown to work at 10.6 μm . The waveguides were obtained by deposition of thick films (up to 15 μm) on polished As_2S_3 glass substrate by thermal evaporation. The films were proved to be homogeneous, dense, adhesive to the chalcogenide substrate and transparent up to 18 micrometers. M-lines measurements at 10.6 μm highlighted the presence of several guided mode lines, proving that the manufactured structures behaved as waveguides and allowed us to measure the refractive index of the layers, i.e. 2.689 ± 0.077 , 2.719 ± 0.003 and 2.821 ± 0.005 were measured for the As_2Se_3 , TeAs_4Se_5 , and $\text{Te}_2\text{As}_3\text{Se}_5$ films, respectively.

(Received August 25, 2005; accepted September 22, 2005)

Keywords: Selenide and telluride thick films, RF-Sputtering, Thermal evaporation, Optical Characterisation, m-lines measurements, Thermal infrared waveguides

1. Introduction

Due to their transparency in the infrared, up to 20 micrometers for few telluride compositions, their high refractive index, their photosensitivity and their ease of preparation in thin film form, chalcogenide glasses appear as good potential candidates for integrated optics and technological applications related to detection in the mid-infrared spectral domain. The papers dealing with these materials in bulk or thin film form have been growing for the past few years [1-4]. In particular some concern environmental metrology [5-7] and others spatial interferometry [8-9] for example. Since a recent date, astronomical interferometry has indeed tackled the question of the direct detection of exo-planetary systems with the ESA *Darwin* mission [10] as a major planned project. The very faint angular separation between an earth-like planet and its parent star as well as the very high contrast between the two bodies has plead in favour of a nulling interferometry mission in the mid-infrared range [4 – 20 micrometers] [10]. In a recent time, the use of single-mode integrated optics (IO) in the near-infrared [11] has shown that this solution was an excellent alternative to bulk optics systems, both for the reduced complexity in the beam combination system and for its features of modal filtering, which is mandatory for nulling interferometry [12]. The opportunity to implement this kind of solution for the *Darwin* mission has then a great interest. To date, single-mode integrated optics is limited to the near infrared windows H and K due to the silica transmission window. It is thus directly incompatible with the will of the *Darwin* mission. Therefore, the development of single-mode integrated optics components working in the whole

* Corresponding author: cvigreux@lpmc.univ-montp2.fr

range [4 μm – 20 μm] is required. One of the promising possibilities to extend the IO concept to the mid-infrared is to use chalcogenide glasses.

The objective of the present work is to validate chalcogenide technology at 10 micrometers. The possibility of depositing some 10 μm -guiding thick layers of different chalcogenide glasses was thus investigated. Three compositions were selected: As_2Se_3 , $\text{Te}_2\text{As}_3\text{Se}_5$ and TeAs_4Se_5 . Their transmission domain is known to extend up to 16 micrometers for the first one, and to 18 microns for the other two [13-14].

2. Experimental

2.1. Thick film manufacturing process

The $\text{Te}_2\text{As}_3\text{Se}_5$ and TeAs_4Se_5 glasses were elaborated using the well-known melt-quenching method, from commercial elemental precursors (Te, As, Se). The chemicals were not further purified in-house before being batched into quartz ampoules in a glove box under a dry argon atmosphere. The ampoules containing the glass batch were evacuated to approximately 10^{-3} Pa, sealed using an oxygen-methane flame and then placed in a furnace. The batches were melted at 600 °C, annealed at 145 °C for $\text{Te}_2\text{As}_3\text{Se}_5$ and 170 °C for TeAs_4Se_5 (approximately 10 °C above the glass transition temperature T_g of the glasses), and cooled slowly down to room temperature. The whole process took approximately 3 days.

Some $\text{Te}_2\text{As}_3\text{Se}_5$ and TeAs_4Se_5 films were deposited by RF-sputtering from bulk glass targets. These targets were obtained from the previously elaborated glasses. The latter were cut in rods of 0.5 cm in length and 2.5 cm in diameter. Before the deposition, the chamber was evacuated down to approximately 10^{-4} Pa to avoid ambient contamination. An operating argon pressure of 5 Pa was used. A low RF power of 20 W was imposed because of the dielectric character of the chalcogenide glasses. The deposition rate was comprised between 0.05 and 0.1 $\mu\text{m}\cdot\text{h}^{-1}$ depending on the composition. Substrates were microscope slides. Before being introduced in the vacuum chamber, they were cleaned with a commercial DECON detergent in an ultrasonic bath, rinsed in alcohol and dried with dry air. The films were annealed at 10 °C below their glass transition temperatures T_g . The RF-sputtered films will be noted RF-TAS1 and RF-TAS2 for TeAs_4Se_5 and $\text{Te}_2\text{As}_3\text{Se}_5$, respectively.

Some As_2Se_3 , $\text{Te}_2\text{As}_3\text{Se}_5$ and TeAs_4Se_5 films were deposited by thermal evaporation from ALDRICH commercial As_2Se_3 and home made $\text{Te}_2\text{As}_3\text{Se}_5$ and TeAs_4Se_5 powders. The powder weight was chosen in order to obtain films of about 10 microns in thickness. Before the deposition, the chamber was evacuated down to approximately 10^{-4} Pa to avoid ambient contamination. A growing intensity was then applied. Three types of substrates were used : (i) microscope slides; (ii) pieces (1 \times 1 cm^2) of polished As_2S_3 bulk glass rinsed in alcohol and dried with dry air and (iii) commercial targets (5 cm in diameter and 5 mm in thickness) of polished As_2S_3 bulk glass also rinsed in alcohol and dried with dry air. The thermal evaporated films will be noted EV-AS, EV-TAS1 and EV-TAS2 for As_2Se_3 , TeAs_4Se_5 and $\text{Te}_2\text{As}_3\text{Se}_5$, respectively.

2.2. Characterisation of the thick films: physical and optical parameters

The glass transition temperature of the TeAs_4Se_5 and $\text{Te}_2\text{As}_3\text{Se}_5$ bulk glasses was measured thanks to a SETARAM DSC 121. The transparency of the bulk glasses was checked using a PERKIN ELMER Spectrum One in the range 5000-400 cm^{-1} . The adhesion of the films on the substrates was checked by the classical adhesive tape test. The film thickness was estimated by profilometry (using a DEKTAK 3 VEECO). The aspect and roughness of the film surface were inspected using a DIGITAL INSTRUMENTS D3100 Atomic Force Microscopy. The film cross-sections were investigated thanks to an HITACHI Scanning Electron Microscopy. The composition of the TeAs_4Se_5 and $\text{Te}_2\text{As}_3\text{Se}_5$ bulk glasses and the composition of the RF-sputtered or thermal evaporated films were analysed thanks to an OXFORD EDS ISIS300 installed on a CAMBRIDGE

SEM S360. The film refractive index at $1.5\ \mu\text{m}$ and optical band gap were estimated from the optical transmittance spectra recorded with an UV-vis-NIR spectrophotometer (CARY 50 VARIAN) in the range $400\ \text{nm} - 3000\ \text{nm}$.

2.3. Characterisation of the thick films: modal behaviour in the near and mid-infrared

To assess that the manufactured films can behave as slab waveguides, the *m*-lines method [15-17] was implemented at the wavelength $\lambda = 10.6\ \mu\text{m}$. The *m*-lines experiment is routinely used to characterise thin films in the visible and near-infrared [17] but it represents a novel and useful instrumental tool for mid-infrared characterisation of 1-dimensional slab waveguides.

The *m*-lines method is based on prism coupling theory: a prism is placed on the surface of the planar waveguides and brought in close contact with the slab through a pushing screw, creating a small air gap (or optical contact) between the slab and the prism surface. If the prism refractive index is higher than the film one and if the conditions of total reflection at the base of the prism are fulfilled, an evanescent field exists in the air gap and light could be coupled onto the existing propagation modes of the waveguide similarly to a tunnelling effect. When a beam is focalised on the optical contact, only specific angular directions of the incoming rays may correspond to the excitement of potential propagation modes. This situation is called “phase matching conditions”. The rays matching this case will thus not be reflected at the base of the prism. This will result in missing black lines (“*m*-lines”) in the reflected beam. Figure 1 provides a schematic diagram of the prism coupling principle. The observation of black lines first ensures that propagation modes exist in the slab waveguide and that they can be excited, providing a proof of the modal behaviour of the sample. In addition, the *m*-lines experiment allows measuring the refractive index of the thin layer and its thickness through a methodology detailed in [16]. The *m*-lines experiment provides a local measurement of the optical parameters of the layer over an area which is of the size of the optical contact (typically $0.25\ \text{mm}^2$) with accuracies of 0.001 on the refractive index and $0.5\ \mu\text{m}$ on the thickness. A complete description of the *m*-lines procedure and measurements on selenide and telluride thick films will be presented in a forthcoming paper (Labadie et al., 2005). *M*-lines measurements were first performed at $1.196\ \mu\text{m}$ and $1.55\ \mu\text{m}$ using a silicon prism in order to benefit from the comparison with data obtained by spectrophotometry. Then, the measurements were pursued in the mid-infrared at $10.6\ \mu\text{m}$ using a germanium prism.

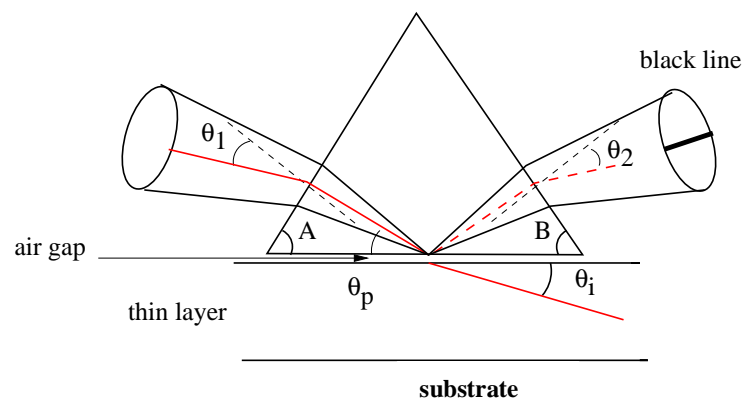


Fig. 1. Schematic of *m*-lines experiment principle. The incident focalized beam contains a ray with angular position θ_1 that fills the phase matching conditions with a propagation mode of the slab waveguide. The coupling process into the waveguide results in a black line in the output beam that coincides with missing energy. The measurement of the black line angular position provides the value of the corresponding mode index.

3. Results and discussion

3.1. Bulk glass characterisation

The $\text{Te}_2\text{As}_3\text{Se}_5$ and TeAs_4Se_5 bulk glasses were amorphous and characterised by glass transition temperatures T_g of 143 °C and 170 °C, respectively. These values are to be compared with the literature ones which are 137 °C [18] and 157 °C [19], respectively. The transparency domain for $\text{Te}_2\text{As}_3\text{Se}_5$ and TeAs_4Se_5 glasses was checked by transmission measurements in the infrared region (Fig. 2).

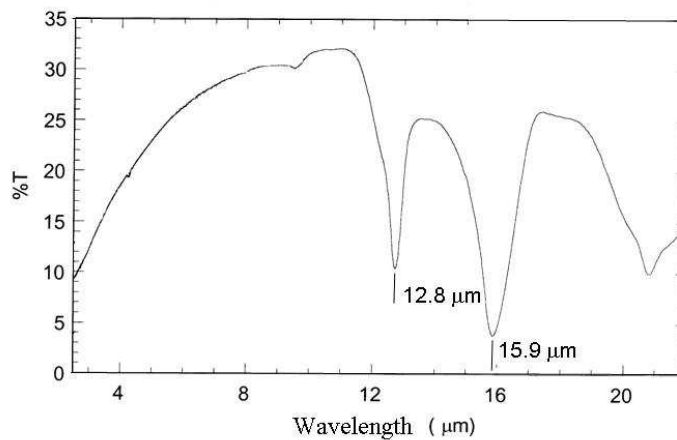


Fig. 2. Transmission spectrum of the TAS1 bulk glass.

If transmission until 18 micrometers was obtained, as predicted by literature [13-14], it can be noted that transmission percentage does not exceed 35 %. This result can be explained taking into account the high TAS glass refractive index, which involves some important losses by reflection at the interfaces of the air. In addition, some important absorption bands were observed around 12.8 and 15.9 micrometers, which were expected taking into account the absence of purification of the elemental precursors and attributed to As-O bonds in As_2O_3 and As-O-As bonds, respectively [20-23]. The presence of oxygen was indeed detected during the EDS measurements. However owing to the very small quantity it has not been taken into account in the calculation of the composition of the two bulk glasses given in Table 1.

Table 1. Composition of the $\text{Te}_2\text{As}_3\text{Se}_5$ and TeAs_4Se_5 glasses as calculated from EDS experiments.

Glass	$\text{Te}_2\text{As}_3\text{Se}_5$	TeAs_4Se_5
At. % in Te	20.6	10.0
At. % in As	30.7	41.1
At. % in Se	48.7	48.9

3.2. Thick film characterisation

The adhesion of the films on the substrates was checked by the classical adhesive tape test. All the RF sputtered thin films were shown to be adhesive to the microscope slides, which was not the case for the thermal evaporated thick films. This result can be understood by the high thickness of the evaporated films which probably induced high stress at the interface. On the other hand, the thermal evaporated thick films were very adhesive on the As_2S_3 bulk glass substrates.

The films deposited on microscope slides were striped down to the substrate and the profile of the stripe was analysed by profilometry. The RF-TAS1 and RF-TAS2 sputtered films were characterised by a thickness of about 0.37 μm and 0.45 μm , respectively. These thicknesses were obtained after 6 hours of deposition. RF-sputtering is thus limited for an application such as spatial interferometry since layers of about 10 micrometers are required. The EV-AS, EV-TAS1 and EV-TAS2 film thicknesses were comprised between 8 and 15 micrometers. The deposition process took 10 minutes approximately.

Whatever the deposition method, thickness was shown to be not homogeneous all over the sample: it is maximum in the centre and decreases as the measured point moves far from it. This result was expected taking into account the fact that the deposition was performed without any rotation of the substrate. The experimental points and the calculated profiles obtained for a 9 micrometers thick EV-TAS2 film are given in Fig. 3.

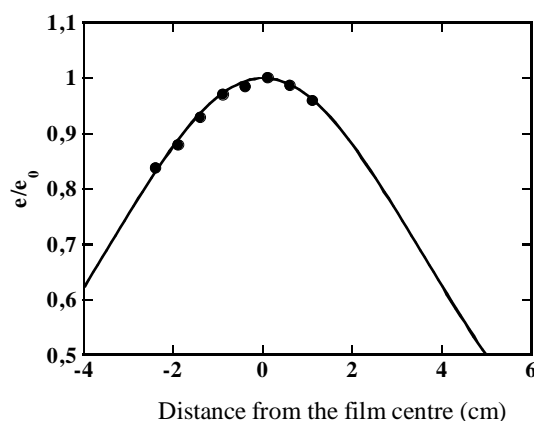


Fig. 3. Thickness measured at different points of a EV-TAS2 film compared to the thickness in the film centre (e_0), versus the distance between the measured points and the centre. The calculated curve was obtained applying a cosinusoidal law.

The RF sputtered films were shown to have a column-like structure. This structure can be explained taking into account the Thornton Zone Diagram [24], the rather high glass transition temperature of the selected telluride materials and the deposition conditions (pressure between 1 and 10 Pa, not-heated substrates). Indeed, three-dimensional nucleation is expected to be the dominant mechanism of film formation in the absence of substrate heating. Therefore, the film growth on the glass substrate most likely forms by the coalescence of islands from nucleation. In order to make the column-like structure disappear, and to get denser films, they were annealed at $T_g + 10^\circ\text{C}$. But the opposite result was obtained: the column-like structure persisted and the gathering of the columns in clusters of bigger size was responsible for an increase in the porosity, as illustrated in Fig. 4.

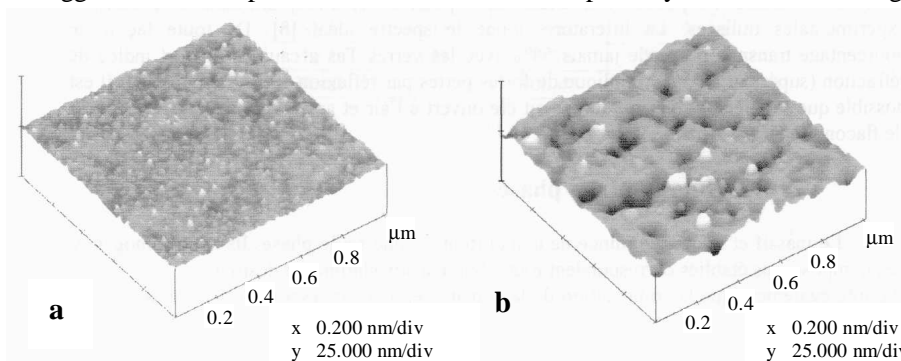


Fig. 4. Three-dimensional AFM pictures of a 0.45 micron thick RF-TAS2 film: a) before annealing; b) after annealing.

This result was already observed in previous work [25]. Furthermore it was shown that the increase in porosity was responsible for a decrease in the refractive index of the films.

No column-like structure was observed in the case of the thermal evaporated films, as shown in the SEM pictures of the EV-TAS1 and EV-TAS2 film cross-sections given in Fig. 5. The layers seem to be dense, at the opposite of the layers obtained by RF sputtering.

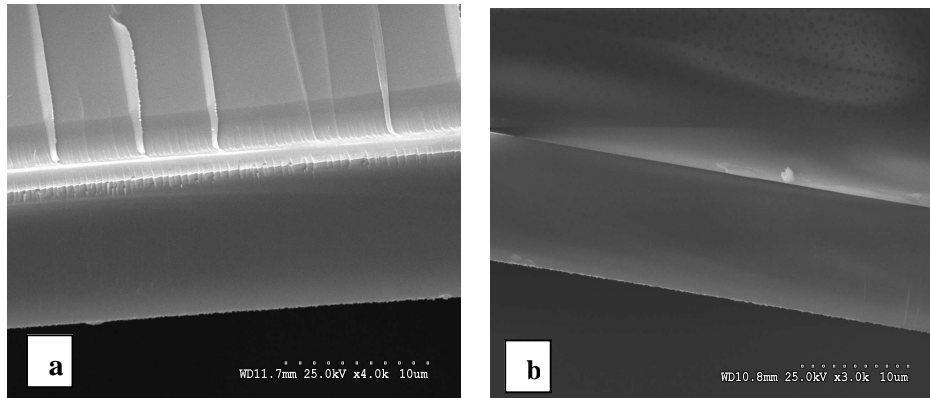


Fig. 5. SEM pictures of the a) 9.2 μm thick $\text{Te}_2\text{As}_3\text{Se}_5$ and b) 10.1 μm thick TeAs_4Se_5 film cross-sections.

The roughness of the EV-TAS1 and EV-TAS2 films was comprised between 10 and 17 nanometers according to an AFM study. It is to be noted that these layers present a mirror aspect, as shown in Fig. 6.



Fig. 6. Photos of a 10.1 micron thick EV-TAS1 film deposited on a As_2S_3 commercial target of 5 cm in diameter and further polished down to 0.2 micron.

The compositions of the telluride films are given in Table 2. It can be noted that the film compositions are not so far from the ones of the bulk glasses, whatever the deposition method. In the case of RF-sputtering, this result is not so unexpected since it is a characteristics of the method to allow the elaboration of layers with composition close to the one of the target. In the case of thermal evaporation, which is usually not advised to obtain multi-components films, such a result could be obtained thanks to the relatively close vapour pressures of the three elements Te, As and Se, i.e. 23.1 Pa at 449 $^{\circ}\text{C}$, 15.8 Pa at 300 $^{\circ}\text{C}$ and 31.6 Pa at 300 $^{\circ}\text{C}$, respectively [26-27].

Table 2. Composition of the telluride films.

Glass	RF-TAS2	RF-TAS1	EV-TAS2	EV-TAS1
At. % in Te	21.0	11.2	23.1	11.1
At. % in As	29.8	39.4	30.9	40.9
At. % in Se	49.2	49.4	46.0	48.0

Only the thermal evaporated films were studied in term of optical characterisation. Indeed it was already shown that the columnar structure of the RF-sputtered chalcogenide films, persisting after annealing, was responsible for a high porosity in the films and a decrease in the effective refractive index compared to the one of the corresponding bulk [25]. The RF-sputtering was thus discarded for the concerned application. On the contrary, the absence of column-like structure justified an optical study of the thermal evaporated films. The refractive index at 1.5 μm and the optical band gap of the evaporated films deposited on microscope slides were estimated from the optical transmission spectra in the 400-3000 nm range. A typical optical transmission spectrum is shown in Fig. 7.

The optical band gaps were estimated to be 671 nm, 838 nm and 924 nm for the EV-AS, EV-TAS1 and EV-TAS2 films, respectively. The refractive index at 1.5 micrometers was estimated considering successive maxima in the curve around 1500 nm. This method is not very precise, since the thickness of the film has to be known with precision whereas it is not homogeneous all over the sample. Values comprised between 2.7 and 2.8 at 1.5 micrometers were obtained for the three compositions. It can be noted that the estimated values are quite close to the ones of the bulk glasses (around 2.8 at 1.55 micrometers [28] and 2.8014 at 3 μm [value given by VITRON, which provides some As_2Se_3 targets] for the AS and 2.8 at 1.55 micrometers for TAS2 bulk glass [29]).

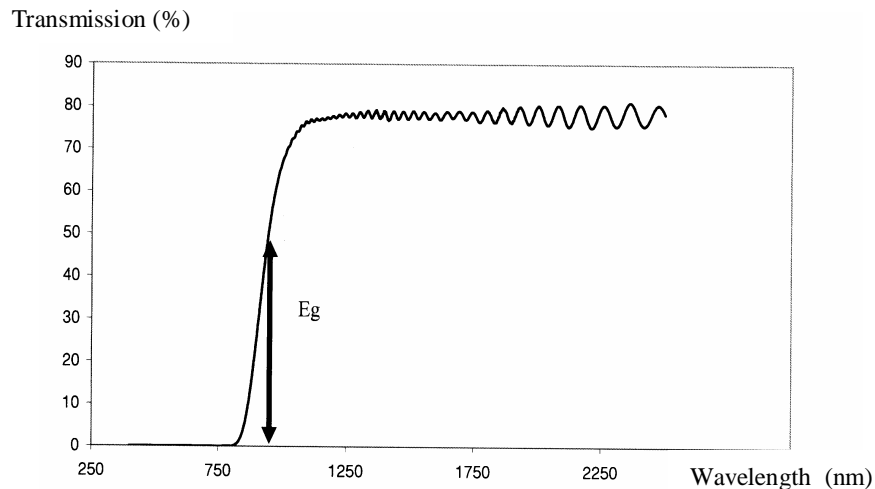


Fig. 7. UV-vis-NIR optical transmission spectrum recorded for a 9.2 micron thick EV-TAS2 film.

This can be related to the poor porosity revealed by the SEM pictures (Fig. 4). Indeed according to Kinoshita and Nishibori relationship (1) the effective refractive index of the film n is close to the refractive index of the bulk glass n_s , when the porosity p is low [30].

$$n = (1-p)n_s + pn_v \quad (1)$$

where n is the effective refractive index, n_v the refractive index of the empty areas, n_s the one of the material, and p the porosity.

To end, the thermal evaporated films deposited on As_2S_3 bulk glass substrates were characterised by the m -lines method. The EV-AS films were characterised in the near-infrared (1.196 μm and 1.55 μm) and the mid-infrared (10.6 μm). The EV-TAS1 and EV-TAS2 films were only characterised in the mid-infrared. In all cases, the simple observation of mode lines proved that the manufactured structures behaved as waveguides with the fulfilled condition $n_{\text{film}} > n_{\text{substrate}}$. The observation of several mode lines clearly revealed a multi-mode behaviour of those samples. In Table 3 are reported the extracted values of refractive index and thickness of the different films. The reported results are made for TE polarisation. This information is of major importance since it will now allow us to calculate the guide dimensions of the further structures in order to achieve 1-dimension single-mode waveguides.

Table 3. Refractive index and thickness measured by the m -lines method for different thermal evaporated films deposited on As_2S_3 bulk glass substrates. Note that the refractive index of these substrates is 2.47 at 1.1966 μm , 2.438 at 1.55 μm and 2.38 at 10.6 μm . For sample EV-AS, the same thickness is measured with 0.5 μm accuracy since the m -lines measurement was performed on the same part of the film.

Sample	EV-AS			EV-TAS1	EV-TAS2
λ (μm)	1.196	1.55	10.6	10.6	10.6
Index n	$2.776 \pm .007$	$2.740 \pm .0077$	$2.689 \pm .0077$	$2.719 \pm .003$	$2.821 \pm .005$
e (μm)	13.2 ± 0.6	13.3 ± 0.6	13.3 ± 0.5	10.0 ± 0.2	8.8 ± 0.2

The value of 2.689 ± 0.0077 at 10,6 microns for the EV-AS film is to be compared to that for the bulk glass, which is 2.7775 at 10 μm [value given by VITRON]. According to Eq.1, it would correspond to a porosity of 5 %, approximately.

4. Conclusion

Three selenide or telluride glasses being potential candidates for the realisation of waveguides working at 10 micrometers were studied: As_2Se_3 , $\text{Te}_2\text{As}_3\text{Se}_5$ and TeAs_4Se_5 . The bulk $\text{Te}_2\text{As}_3\text{Se}_5$ and TeAs_4Se_5 glasses were elaborated by the classical melt-quenching method. The $\text{Te}_2\text{As}_3\text{Se}_5$ and TeAs_4Se_5 glasses were shown to be characterised by a glass transition temperature of about 143 $^\circ\text{C}$ and 170 $^\circ\text{C}$, respectively. The absence of purification of the elemental precursors was responsible for some absorption bands around 13 and 15 micrometers, due to As-O bonds.

The films were deposited by two different methods: RF sputtering and thermal evaporation. RF sputtering [31] was rapidly discarded since the deposition rate is very low and the sputtered dielectric films have a columnar structure, resulting in a high porosity and low refractive index. Thermal evaporation allowed to obtain layers with thicknesses comprised between 8 and 15 micrometers. These layers are dense and adhesive to polished As_2S_3 glass substrates. The vapour pressures of the three elements Te, As and Se being similar, the composition of the films was very close to the one of the bulk glasses. Thanks to transmission spectra recorded in the [400-3000 nm] range, the refractive index was estimated to be comprised between 2.7 and 2.8 at 1.5 microns, whatever the composition. In the case of the As_2Se_3 thick films, m -lines experiments confirmed such a value, since a refractive index of 2.740 ± 0.077 at 1.55 μm was obtained. The m -lines measurements at 10.6 μm gave very encouraging results, since the observation of several mode lines proved the waveguide behaviour of the structures. Refractive indexes of 2.689 ± 0.077 , 2.719 ± 0.003 and 2.821 ± 0.005 were measured for the As_2Se_3 , TeAs_4Se_5 , and $\text{Te}_2\text{As}_3\text{Se}_5$ films, respectively.

Our objective was to prove the feasibility of waveguides based on selenide or telluride glasses and able to work in the mid-infrared. The first results are very encouraging, since they prove that it is possible to deposit thick (up to 15 μm) adhesive waveguiding films of good optical quality

by thermal evaporation. The observation of several mode lines highlighted a multi-mode behaviour and the knowledge of the refractive index at 10.6 μm will allow for the optimisation of the guide geometry in order to observe a single-mode one.

Acknowledgments

The authors are grateful to V. Ranieri, V. Boulenc, S. Monclar and F. Vial for their contribution to the work and to Dr. Amal Chabli for her precious help in the m-lines measurements. The authors thanks the IMEP-INPG and the European Space Agency for financial support and interest in the work.

References

- [1] D. A. Turnbull, J. S. Sanghera, V. Q. Nguyen, I.D. Aggarwal, *Mater. Lett.* **58**(1-2), 51 (2004).
- [2] S. Ramachandran, S. G. Bishop, *Appl. Phys. Lett.* **74**, 13 (1999).
- [3] M. Martino, A. P. Caricato, M. Fernandez, G. Leggieri, A. Jha, M. Ferrari, M. Mattarelli, *Thin Solid Films* **433**, 39 (2003).
- [4] P. Nagels, E. Sleenckx, R. Callaerts, E. Marquez, J. M. Gonzales-Leal, A. M. Bernal-Oliva, *Solid States Ionics* **102**(7), 539 (1997).
- [5] J. Keirsse, C. Boussard-Plédel, O. Loreal, O. Sire, B. Bureau, B. Turlin, P. Leroyer, J. Lucas, *J. of Non-Cryst. Solids* **326/327**, 430 (2003).
- [6] V. Balan, C. Vigreux, A. Pradel, A. Llobera, C. Dominguez, M. I. Alonso, M. Garriga, *J. of Non-Cryst. Solids* **326/327**, 455 (2003).
- [7] D. Le Coq, C. Boussard-Plédel, G. Fonteneau, T. Pain, B. Bureau, J. L. Adam, *Materials Research Bulletin* **38**(13), 174 (2003).
- [8] E. Laurent, I. Schanen, F. Malbet, G. Taillades, *Astronomical Telescopes and Instrumentation, Interferometry in Optical Astronomy*, Munich, Germany, March 27-31, 2000, *Proc. SPIE Vol.* **4006**, 1090 (2000).
- [9] E. Laurent, P. Kern, I. Schanen, V. Balan, C. Vigreux, A. Pradel, R. Romestain, S. Setzu, P. Labeye, K. Perraut, and P. Benech, *Astronomical Telescopes and Instrumentation, Interferometry in Optical Astronomy*, Hawaii, U.S.A., August 22-28, 2003, *Proc. SPIE* **4838**, 1344 (2003).
- [10] M. Fridlund, in *ASP Conf. Ser.* 213, *Bioastronomy* **99**, 167 (2000).
- [11] J.-P. Berger et al., *Astronomy and Astrophysics*, **376**, L31 (2001).
- [12] M. Ollivier et al., *Applied Optics* **36**, 5340 (1997).
- [13] V. S. Shiryaev, J.-L. Adam, X. H. Zhang, C. Boussard-Plédel, J. Lucas, M. F. Churbanov, *J. of Non-Crystalline Solids* **336**, 113 (2004).
- [14] S. Hocde, "Fibres optiques en verre infrarouge, application en chimie et biologie", Thèse, Université de Rennes I (2000).
- [15] P. K. Tien, R. Ulrich, R. J. Martin, *Applied Physics Letters* **14**, 291 (1969).
- [16] R. Ulrich, R. Torge, *Applied Optics* **12**, 2901 (1973).
- [17] J. M. White, P. F. Heidrich, *Applied Optics* **15**, 151 (1976).
- [18] K. Michel, B. Bureau, C. Pouvreau, J. C. Sangleboeuf, C. Boussard-Plédel, T. Jouan, T. Rouxel, J. -L. Adam, K. Staubmann, H. Steinner et al., *J. of Non-Cryst. Solids* **326-327** 434 (2003).
- [19] D. D. Thornburg, *J. of Electr. Mater.* **2**(4) (1973).
- [20] T. Kanamori, Y. Terunuma, S. Takahashi, T. Miyashita, *J. of Non-Cryst. Solids* **69**, 231 (1985).
- [21] C. T. Moynihan, P. B. Macedo, M. S. Maklad, R. K. Mohr, R. E. Howard, *J. of Non-Cryst. Solids* **17**, 369 (1975).
- [22] D. S. Ma, P. S. Danielson, C. T. Moynihan, *J. of Non-Cryst. Solids* **37**, 181 (1980).
- [23] J. Nishii, T. Yamashita, T. Yamagishi, *J. Mater. Sci.* **24**, 4293 (1989).
- [24] J. A. Thornton, *J. Vac. Sci. Technol.* **11**, 666 (1974).
- [25] V. Balan, C. Vigreux, A. Pradel, *J. Optoelectron. Adv. Mater.* **6**(3), 875 (2004).

- [26] A. B. Seddon, Proc. 9th International Symposium on non-oxide glasses, Hangzhou, China 14 (1994).
- [27] D. Lezal, B. Petrovska, G. Kuncova, M. Pospisilova, J. Gotz, Proc. SPIE **799**, 44 (1987).
- [28] J. M. Laniel, J. M. Ménard, K. Turcotte, A. Villeneuve, R. Vallée, C. Lopez, K. A. Richardson, J. of Non-Cryst. Solids **328**, 183 (2003).
- [29] A. R. Hilton, Proc. SPIE Infrared Fiber Optics III, **1591**, 34 (1991).
- [30] K. Kinoshita, M. Nishibori in: A. Richardt, A.-M. Durand, Les interactions ions énergétiques-solides, In Fine, Paris, (1997) 357.
- [31] V. Balan, C. Vigreux, A. Pradel, J. Optoelectron. Adv. Mater. **6**(3), 875 (2004).